基于酰胺−吡唑双功能配体的钯配位"夹子"的自组装及其催化性能

胡效鹏　　王志锋　　于澍燕*

(北京工业大学环境与生命学部，绿色催化与分离北京市重点实验室，

北京工业大学环境安全与生物效应卓越中心，自组装化学实验室，北京　100124)

摘要：利用配位驱动吡唑基配体在溶液中自发去质子自组装的方法，用金属转子[(bpy)$_2$Pd$_2$(NO$_3$)$_2$](NO$_3$)$_2$、[(dmbpy)$_2$Pd$_2$(NO$_3$)$_2$](NO$_3$)$_2$(bpy=2，2′-联吡啶，dmbpy=4，4′-二甲基-2，2′-联吡啶)和酰胺−吡唑双功能配体(HL^1、HL^2)合成了含有Pd(Ⅱ)⋯Pd(Ⅱ)相互作用的[Pd$_2$L$_2$]$^{2+}$类型的吡唑基双钯(Ⅱ，Ⅱ)"夹子"**C1~C4**。利用^{1}H和^{13}C NMR、ESI-MS、红外光谱和X射线单晶衍射等测试手段对配合物**C1~C4**的结构进行了表征。同时，合成的夹子状双金属配合物对Suzuki-coupling反应均表现出较好的催化活性。

关键词：自组装；双钯(Ⅱ)"夹子"；催化；Suzuki-coupling反应

Palladium-Based Coordination "Clips" with Carboxamide-Pyrazolate Ditopic Ligands: Self-Assembly and Catalytic Properties

HU Xiao-Peng　　WANG Zhi-Feng　　YU Shu-Yan*

(*Laboratory for Self-Assembly Chemistry, Center of Excellence for Environmental Safety and Biological Effects,*

Beijing Key Laboratory for Green Catalysis and Separation, Department of Environment and Life,

Beijing University of Technology, Beijing 100124, *China*)

Abstract: Two dipalladium complexes [(bpy)$_2$Pd$_2$(NO$_3$)$_2$](NO$_3$)$_2$, [(dmbpy)$_2$Pd$_2$(NO$_3$)$_2$](NO$_3$)$_2$ (bpy=2,2-bipyridine, dmbpy=4,4′-dimethyl-2,2-bipyridine) were used as "clips" to coordinate with ditopic pyrazolate ligands (HL^1, HL^2), leading to the formation of [Pd$_2$L$_2$]$^{2-}$-type dinuclear coordination "clips" with strong intramolecular Pd(Ⅱ)⋯Pd(Ⅱ) bonding interaction through a spontaneous deprotonation of the pyrazole ligands in aqueous solution. Such well-defined complexes **C1~C4** have been characterized by single-crystal X-ray diffraction analysis, elemental analysis, ^{1}H and ^{13}C NMR, electrospray ionization mass spectrometry (ESI-MS) and IR spectroscopy. Furthermore, all these clip-like dipalladium(Ⅱ) complexes exhibited highly catalytic activities towards Suzuki-coupling reaction under mild conditions. CCDC: 2060495, **C1·**2NO$_3^-$.

Keywords: self-assembly; dipalladium(Ⅱ) "clips"; catalysis; Suzuki-coupling reaction

　　Coordination-driven self-assembly continues to spark the vibrant field of supramolecular chemistry, owing to its predictability for the construction of elegant functional structures[1-3]. Over the past decades, several metal-directed assembly strategies have been developed to achieve well-defined supramolecular architectures, such as clips, squares, cages, grids, and capsules[4-7]. With the advance of the field, increasing efforts have now been devoted to design architectures with diverse functions and applications, such as cataly-

sis, guests binding, drug delivery, separation, stimuli-responsive materials and cancer theranostics[8-10]. Among these efforts, the selection of a suitable strategy for construction of ensembles with controllable shapes and predictable functions is still drawing particular attentions[11-14].

Since the recognition of the multiple bonding $[Re_2Cl_8]^{2-}$ by F. A. Cotton in 1960s, the chemistry of the dimetal-or multimetal-centered compounds have drawn increasing interest due to their structural diversity, rich physical properties and potential applications in catalysis, magnetic coupling and functional materials[15-17]. Recently, the utilization of dimetal units as

directional building blocks and the bidentate ligands as linkers has extended such chemistry toward the emerging field of metallo-supramolecular architecture[18-19].

Meanwhile, the transition metal palladium complexes have been a hot topic in the area of Suzuki-coupling reaction. The mononuclear palladium catalysis had played a crucial role in synthetic organic chemistry for Suzuki-coupling reaction. In the past few years, considerable attention has been paid to functional metal-organic assemblies that show promise in catalysis[20-21]. Especially, palladium was employed in Suzuki-coupling reaction for their high stability and

(ⅰ) H_2O, acetone, reflux; (ⅱ) KPF_6
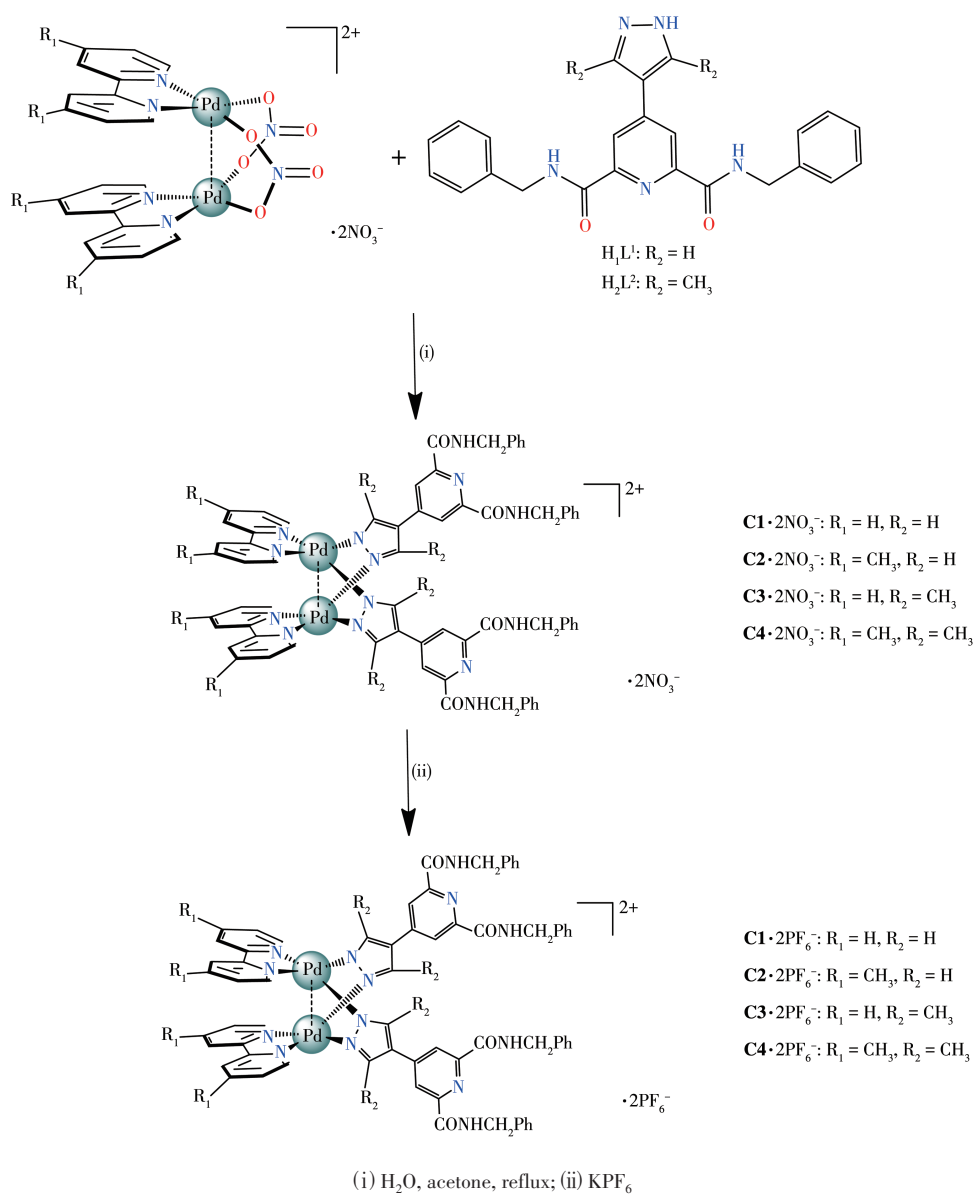
Scheme 1   Schematic illustration of self-assembly of dipalladium "clips" $C1 \cdot 2NO_3^- \sim C4 \cdot 2NO_3^-$ and $C1 \cdot 2PF_6^- \sim C4 \cdot 2PF_6^-$

remarkable efficiency. In our search for new coordination motifs as building blocks in supramolecular architecture, we noticed that the versatile ligands 1H-bipyrazoles could be good alternatives for the widely used carboxylates or other bidentate chelating ligands in binding dimetal centers[22-24]. Considering the variety of potential catalysis applications of pyrazolate-bridged multimetal coordination compounds, we studied the self-assembly of metallo-clips with bifunctional ligand.

In our group, a series of novel metallosupromolecules have been successfully synthesized through the stepwise ligand substitution reaction of different pyrazolate ligands with bimetal motifs $[(N^{\wedge}N)_2Pd_2(NO_3)_2]$ $(NO_3)_2$ (where $N^{\wedge}N$=2,2′-bipyridine, bpy; 4,4′-dimethyl-2,2′-bipyridine, dmbpy)[25-26]. In this work, we successfully synthesized a series of functional $[M_2L_2]^{2+}$-type coordination "clips" **C1~C4** using a novel kind of carboxamide-pyrazolate ditopic ligands with two dipalladium building units $[(N^{\wedge}N)_2Pd_2(NO_3)_2]$ $(NO_3)_2$, as shown in Scheme 1. The supramolecular assemblies have been intensively studied by NMR spectroscopy, electrospray ionization mass spectrometry (ESI-MS) in solution and by IR spectroscopy, X-ray crystallographic analysis in the solid state.

1　Experimental

1.1　Reagents and physical instruments

All chemicals and solvents were of AR grade and used without further purification. Carbon, hydrogen and nitrogen were determined using an Elementar Vario EL elemental analyzer. ^1H and ^{13}C NMR spectra were recorded on Bruker AV 400 MHz spectrometers.

The ESI-MS were recorded on Octant TOF LC-plus 4G mass spectrometer. The FT-IR spectra were recorded as KBr pellets on a Shimadzu IR Prestige-21 spectrometer. Single crystal X-ray diffraction analysis were recorded on Bruker apex Ⅱ instrument.

1.2　Synthesis and characterization of $C1\cdot2NO_3^-$ $\sim C4\cdot2NO_3^-$ and $C1\cdot2PF_6^-\sim C4\cdot2PF_6^-$

1.2.1　General pyrazole ligand preparation

The pyrazole ligand HL^1 and HL^2 were prepared by using similar methods as described in those works in our group[19,26] (Scheme 2). N^2,N^6-dibenzyl-4-(1H-pyrazol-4-yl)pyridine-2,6-dicarboxamide (HL^1): ^1H NMR (400 MHz, DMSO-d_6, 298 K): δ 4.62 (d, 2H), 7.26 (d, 5H), 8.43 (s, 1H), 8.71(s, 1H), 9.89 (m, 1H), 13.33 (s, 1H). ^{13}C NMR (400MHz, DMSO-d_6, 298 K): δ 164.06, 149.90, 144.28, 139.82, 137.83, 128.84, 127.40, 120.23, 118.72, 42.65; N^2,N^6-dibenzyl-4-(3,5-dimethyl-1H-pyrazol-4-yl)pyridine-2,6-dicarboxamide (HL^2): ^1H NMR (400 MHz, DMSO-d_6, 298 K): δ 2.33 (s, 3H), 4.61 (d, 2H), 7.26 (m, 5H), 8.15(s, 1H), 9.96 (m, 2H), 12.24 (s, 1H). ^{13}C NMR (400 MHz, DMSO-d_6, 298 K): δ 163.94, 149.51, 145.50, 139.87, 128.81, 127.49, 127.28, 123.03, 114.19, 42.66, 12.41.

1.2.2　Synthesis and characterization of $[M_2L_2]^{2+}$-type coordination "clips"

The self-assembly of metallo-clip complexes **C1·** $2NO_3^-$ and **C1·**$2PF_6^-$ are shown in Scheme 1. HL^1 (41.5 mg, 0.1 mmol) was added to a suspension solution of $[(bpy)_2Pd_2(NO_3)_2](NO_3)_2$ (38.7 mg, 0.05 mmol) in H_2O/acetone (1∶4, V/V). The mixture was stirred for 2 h at room temperature, then was heated at 80 ℃ for 6 h to give **C1·**$2NO_3^-$. **C1·**$2NO_3^-$: ^1H NMR (400 MHz,
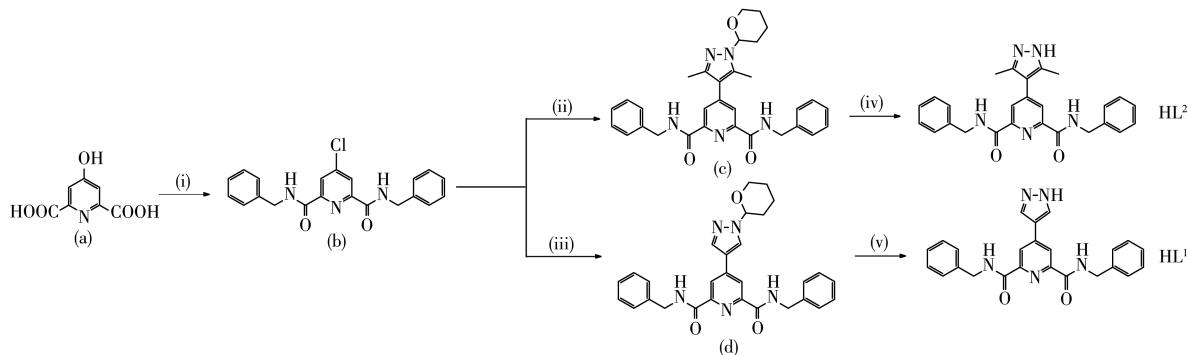
(ⅰ) $POCl_3$, phenylmethanamine, reflux; (ⅱ) Dmtty, K_2CO_3, $Pd(PPh_3)_4$, reflux; (ⅲ) tty, K_2CO_3, $Pd(PPh_3)_4$, reflux; (ⅳ/ⅴ) HCl, methanol, reflux

Scheme 2　Synthesis of HL^1 and HL^2

DMSO-d$_6$, 298 K, ppm): δ 8.73 (t, 1H, bpy-1), 8.48 (d, 1H, bpy-2), 7.78 (d, 1H, bpy-3), 8.33 (t, 1H, bpy-4), 9.88 (t ,1H, L^1-a), 8.95 (s, 1H, L^1-b), 4.61 (s, 2H, L^1-c), 7.31 (t, 2H, L^1-d), 7.32 (d, 2H, L^1-e), 7.26 (m, 1H, L^1-f), 8.48 (s, 1H, L^1-g). ^{13}C NMR (400 MHz, DMSO-d$_6$, 298 K): δ 163.87, 156.30, 151.71, 150.27, 149.94, 142.82, 140.98, 128.85, 127.42, 124.74, 122.74, 122.49, 120.16, 119.53, 42.64. Elemental analysis Calcd. for C$_{68}$H$_{56}$N$_{16}$O$_{10}$Pd$_2$(%): C, 55.56; H, 3.84; N, 15.24. Found (%): C, 55.53; H, 3.85; N, 15.24. The PF$_6^-$ salts of **C1**· 2NO$_3^-$ was obtained by adding ten-fold excess of KPF$_6$ to the solution of **C1**·2NO$_3^-$. The mixture was stirred continuously for 6 h, then the precipitation was filtered, washed with minimum amount of cold water and dried in vacuum as yellow solid. **C1**·2PF$_6^-$ was obtained as yellow needle crystal in quantitative yield (96%, 78.41 mg). **C1**·2PF$_6^-$: ^{1}H NMR (400 MHz, DMSO-d$_6$, 298 K): δ 8.77 (t, 1H, bpy-1), 8.49 (d, 1H, bpy-2), 8.35 (d, 1H, bpy-3), 7.85 (t, 1H, bpy-4), 9.90 (t ,1 H, L^1-a), 8.97 (s, 1H, L^1-b), 4.60 (s, 2H, L^1-c), 7.32 (t, 2H, L^1-d), 7.33 (d, 2H, L^1-e), 7.24 (m, 1H, L^1-f), 8.51 (s, 1H, L^1-g). ^{13}C NMR (400 MHz, CD$_3$CN, 298 K): δ 163.88, 156.49, 151.41, 150.27, 142.75, 142.53, 140.04, 139.89, 129.06, 128.18, 127.71, 124.60, 123.38, 123.16, 43.18. FT-IR (KBr, cm^{-1}): 3 336(s), 3 055(s), 1 680(w), 1 606 (m), 1 520(m), 1 459(s), 1 263(s), 1 176(s), 1 042(m), 709.9(m), 636(s). ESI-MS (CH$_3$CN, *m/z*): Calcd. for [**C1**]$^{2+}$ 673.05, Found: 672.58; Calcd. for [**C1**·PF$_6^-$]$^+$ 1 491.07, Found: 1 490.90. Elemental analysis Calcd. for C$_{68}$H$_{56}$F$_{12}$N$_{14}$O$_4$P$_2$Pd$_2$(%): C, 49.92; H, 3.45; N, 11.99. Found(%): C, 49.92; H, 3.46; N, 11.94.

The similar procedure as employed for **C1**·2NO$_3^-$ and **C1**·2PF$_6^-$ were followed except that [(dmbpy)$_2$Pd$_2$ (NO$_3$)$_2$](NO$_3$)$_2$ (41.4 mg, 0.05 mmol) was used as starting material to give **C2**·2NO$_3^-$ as a light-yellow precipitate (74.6 mg, Yield: 98%), **C2**·2PF$_6^-$ as a light-yellow precipitate (82.0 mg, Yield: 97%). **C2**·2NO$_3^-$: ^{1}H NMR (400 MHz, DMSO-d$_6$, 298 K): δ 8.40 (t, 1H, bpy-1), 8.16 (d, 1H, bpy-2), 7.63 (d, 1H, bpy-3), 2.56 (t, 3H, bpy-4), 9.97 (t ,1 H, L^1-a), 8.92 (s, 1H, L^1-b), 8.59 (s, 2H, L^1-c), 7.31 (t, 2H, L^1-d), 7.30 (d, 2H, L^1-e), 7.26 (m, 1H, L^1-f), 4.60 (s, 2H, L^1-g). ^{13}C NMR (400 MHz, DMSO-d$_6$, 298 K): δ 163.83, 155.80, 155.07, 149.87,

139.75, 128.85, 127.41, 125.13, 122.40, 120.07, 42.62, 21.48. Elemental analysis Calcd. for C$_{72}$H$_{64}$N$_{16}$O$_{10}$Pd$_2$ (%): C, 56.66; H, 4.23; N, 14.68. Found(%): C, 56.64; H, 4.26; N, 14.64. **C2**·2PF$_6^-$: ^{1}H NMR (400 MHz, DMSO, 298 K): δ 8.40 (t, 1H, dmbpy-1), 8.14 (d, 1H, dmbpy-2), 7.62 (d, 1H, dmbpy-3), 2.56 (s, 1H, dmbpy-4), 9.86 (t ,1 H, L^1-a), 8.90 (s, 1H, L^1-b), 8.59 (s, 1H, L^1-c), 7.26 (m, 2H, L^1-d), 7.25 (d, 2H, L^1-e), 7.24 (d, 1H, L^1-f), 4.60 (s, 1H, L^1-g). ^{13}C NMR (400 MHz, DMSO-d$_6$, 298 K): δ 163.84, 155.82, 155.05, 150.76, 149.90, 139.77, 128.84, 127.42, 125.16, 122.76, 122.43, 120.10, 119.55, 42.65, 21.50. FT-IR (KBr, cm^{-1}): 3 364(s), 1 668(w), 1 606(m), 1 532(m), 1 422(m), 1 299(m), 1 237(m), 1 066(m), 992(m), 857(m), 562(s). ESI-MS (CH$_3$CN, *m/z*): Calcd. for [**C2**]$^{2+}$ 701.15, Found: 701.62; Calcd. for [**C2**·PF$_6^-$]$^+$ 1 547.17, Found: 1 547.21. Elemental analysis Calcd. for C$_{72}$H$_{64}$N$_{14}$O$_4$F$_{12}$P$_2$Pd$_2$(%): C, 51.11; H, 3.81; N, 11.59. Found(%): C, 51.14; H, 3.80; N, 11.59.

The similar procedure as employed for **C1**·2NO$_3^-$ and **C1**·2PF$_6^-$ were followed except that [(bpy)$_2$Pd$_2$ (NO$_3$)$_2$](NO$_3$)$_2$ (38.6 mg, 0.05 mmol) and HL^2 (43.6 mg, 0.1 mmol) were used as starting material to give **C3**· 2NO$_3^-$ as a light-yellow precipitate (74.5 mg, Yield: 98%), **C3**·2PF$_6^-$ as a light-yellow precipitate (81.6 mg, Yield: 96%). **C3**·2NO$_3^-$: ^{1}H NMR (400 MHz, DMSO-d$_6$, 298 K): δ 8.48 (t, 1H, bpy-1), 8.27 (d, 1H, bpy-2), 8.26 (d, 1H, bpy-3), 7.78 (t, 1H, bpy-4), 9.95 (t ,1H, L^1-a), 8.75 (s, 1H, L^1-b), 7.34 (s, 2H, L^1-c), 4.64 (t, 2H, L^1-d), 2.61 (d, 3H, L^1-e), 7.33 (m, 2H, L^1-f), 7.26 (s, 1H, L^1-g). ^{13}C NMR (400 MHz, DMSO-d$_6$, 298 K): δ 163.93, 157.25, 151.03, 149.53, 148.82, 144.56, 142.86, 139.77, 128.86, 128.62, 127.45, 127.35, 124.83, 123.71, 42.69, 23.25, 14.02. Elemental analysis Calcd. for C$_{72}$H$_{64}$N$_{16}$O$_{10}$Pd$_2$ (%): C, 56.66; H, 4.23; N, 14.68. Found(%): C, 56.65; H, 4.24; N, 14.66. **C3**·2PF$_6^-$: ^{1}H NMR (400 MHz, CD$_3$CN, 298 K): δ 8.63 (t, 1H, bpy-1), 8.36 (d, 1H, bpy-2), 8.32 (d, 1H, bpy-3), 7.75 (s, 1H, bpy-4), 9.81(s ,1H, L^2-a), 8.74 (s, 1H, L^2-b), 7.31 (m, 2H, L^2-c), 7.27 (d, 2H, L^2-d), 2.69 (s, 3H, L^2-e), 7.27 (d, 2H, L^2-f), 7.19 (s, 1H, L^2-g). ^{13}C NMR (400 MHz, DMSO-d$_6$, 298 K): δ 163.92, 157.25, 151.03, 149.54, 148.82, 144.54, 142.86, 139.78, 128.84, 127.45, 124.84, 123.69, 117.63, 42.69,

14.01. FT-IR (KBr, cm^{-1}): 3 287(s), 3 000(s), 1 657(w), 1 603(m), 1 525(m), 1 425(m), 1 248(m), 832(m), 764 (m), 558(m). ESI-MS (CH$_3$CN, *m/z*): Calcd. for [**C3**]$^{2+}$ 701.15, Found: 701.17; Calcd. for [**C3**·PF$_6^-$]$^+$ 1 547.17, Found: 1 547.21. Elemental analysis Calcd. for C$_{72}$H$_{64}$N$_{14}$O$_4$F$_{12}$P$_2$Pd$_2$(%): C, 51.11; H, 3.81; N, 11.59. Found(%): C, 51.12; H, 3.80; N, 11.58.

　　The similar procedure as employed for **C1**·2NO$_3^-$ and **C1**·2PF$_6^-$ were followed except that [(dmbpy)$_2$Pd$_2$(NO$_3$)$_2$](NO$_3$)$_2$ (41.4 mg, 0.05 mmol) and HL^2 (43.6 mg, 0.1 mmol) were used as starting material to give **C4**·2NO$_3^-$ as a light‐yellow precipitate (78.2 mg, Yield: 99%), **C4**·2PF$_6^-$ as a light‐yellow precipitate (82.1 mg, Yield: 94%). **C4**·2NO$_3^-$: ^{1}H NMR (400 MHz, DMSO‐d$_6$, 298 K): δ 8.24 (t, 1H, bpy‐1), 8.09 (d, 1H, bpy‐2), 7.60 (d, 1H, bpy‐3), 2.57 (t, 3H, bpy‐4), 9.96 (t ,1 H, L^1‐a), 8.59 (s, 1H, L^1‐b), 7.33 (s, 2H, L^1‐c), 4.63 (t, 2H, L^1‐d), 2.57 (d, 3H, L^1‐e), 7.32 (m, 2H, L^1‐f), 7.26 (s, 1H, L^1‐g). ^{13}C NMR (400 MHz, DMSO‐d$_6$, 298 K): δ 163.91, 156.63, 155.25, 150.24, 149.51, 148.66, 144.55, 139.77, 128.85, 127.44, 125.37, 123.66, 117.52, 42.67, 21.55, 14.01. Elemental analysis Calcd. for C$_{76}$H$_{72}$N$_{16}$O$_{10}$Pd$_2$ (%): C, 57.69; H, 4.59; N, 14.16. Found(%): C, 57.67; H, 4.56; N, 14.14. **C4**·2PF$_6^-$: ^{1}H NMR (400 MHz, CD$_3$CN, 298 K): δ 8.21 (t, 1H, bpy‐1), 7.97 (d, 1H, bpy‐2), 7.46 (d, 1H, bpy‐3), 2.55 (s, 1H, bpy‐4), 9.02 (s , 1H, L^2‐a), 8.27 (s, 1H, L^2‐b), 7.35 (t, 2H, L^2‐c), 4.61 (d, 2H, L^2‐d), 2.56 (s, 3H, L^2‐e), 7.32 (t, 2H, L^2‐f), 7.25 (d,

1H, L^2‐g). ^{13}C NMR (400 MHz, DMSO‐d$_6$, 298 K): δ 163.88, 156.49, 151.41, 150.27, 142.75, 142.53, 140.04, 139.89, 129.06, 128.84, 128.18, 127.71, 124.60, 123.38, 123.16, 43.18, 21.05, 14.85. FT-IR (KBr, cm^{-1}): 3 294 (s), 1 656(w), 1 532(m), 1 422(m), 1 249(m), 1 030(s), 821(m), 538(s). ESI-MS (CH$_3$CN, *m/z*): Calcd. for [**C4**]$^{2+}$ 729.15, Found: 729.15; Calcd. for [**C4**·PF$_6^-$]$^+$ 1 603.28, Found: 1 603.29. Elemental analysis Calcd. for C$_{76}$H$_{72}$N$_{14}$F$_{12}$O$_4$P$_2$Pd$_2$(%): C, 52.21; H, 4.15; N, 11.22. Found(%): C,52.23; H, 4.11; N, 11.23.

1.3　X-ray crystallography of complex C1·2NO$_3^-$

　　Single crystals of **C1**·2NO$_3^-$ were obtained by vapor diffusion isopropyl ether into its metanol solu‐ tion. The intensity data collection (single crystals with dimensions of 0.16 mm×0.14 mm×0.12 mm for the complex) was performed on the Bruker Smart APEX Ⅱ CCD diffractometry equipped with graphite monochro‐ mated Mo *Kα* radiation (λ=0.071 073 nm).

　　The structure was solved by direct methods and refined employing full‐matrix least‐squares on F^2 by using SHELXTL program[27] and expanded using Fouri‐ er techniques. The final residuals along with unit cell, space group, data collection, and refinement parame‐ ters are presented in Table 1. The final selected bond length and bond angles for **C1**·2NO$_3^-$ are listed on Table S1 and S2 (Supporting information).

　　CCDC: 2060495, **C1**·2NO$_3^-$.

Table 1　Crystal structure data and refinement parameters for complex C1·2NO$_3^-$

Formula	C$_{68}$H$_{56}$N$_{16}$O$_{10}$Pd$_2$	Z	2
Formula weight	1 470.08	D_c / (Mg·m^{-3})	1.215
Crystal system	Triclinic	Absorption coefficient / mm^{-1}	0.506
Space group	$P\bar{1}$	$F(000)$	1 496
Volume / nm^3	1.925 6(7)	Independent reflection	19 853 (R_{int}=0.027 4, R_σ=0.037 8)
a / nm	0.127 53(2)	Absorption correction	Empirical
b / nm	0.133 84(2)	Data, restraint, parameter	19 853, 0, 865
c / nm	0.246 68(2)	Goodness-of-fit on F^2	1.074
$α$ / (°)	97.372(9)	Final R indices [$I>2σ(I)$]	R_1=0.029 3, wR_2=0.070 4
$β$ / (°)	102.645(9)	R indices (all data)	R_1=0.038 9, wR_2=0.073 4
$γ$ / (°)	97.553(8)	Largest diff. peak and hole / (e·nm^{-3})	600 and −600

1.4　Catalytic activity test

　　To explore the catalytic activity of pyrazolate‐ based dipalladium with weak dinuclear Pd(Ⅱ)···Pd(Ⅱ)

intra‐molecular bonding interaction between two Pd(Ⅱ) centers, different reaction conditions have been tried and the feasible solution was obtained.

In a typical experiment, the iodobenzene (204 mg, 1 mmol), 3,4-dimethoxy benzeneboronic acid (182 mg, 1 mmol), and K_3PO_4 (318.4 mg, 1.5 mmol), or $\mathbf{C1}\cdot 2NO_3^-$ (14.2 mg, 10 μmmol), or $\mathbf{C2}\cdot 2NO_3^-$ (15.2 mg, 10 μmmol), or $\mathbf{C3}\cdot 2NO_3^-$ (15.3 mg, 10 μmmol) and $\mathbf{C4}\cdot 2NO_3^-$ (15.8 mg, 10 μmmol), or $\mathbf{C1}\cdot 2PF_6^-$ (16.3 mg, 10 μmmol), or $\mathbf{C2}\cdot 2PF_6^-$ (16.9 mg, 10 μmmol), or $\mathbf{C3}\cdot 2PF_6^-$ (16.8 mg, 10 μmmol) and $\mathbf{C4}\cdot 2PF_6^-$ (17.4 mg, 10 μmmol) was added into a 100 mL flask. 30 mL 1,4-dioxane was added and the suspension was stirred at under 100 ℃ and nitrogen atmosphere. After the reactant disappeared (the consumption of the starting iodobenzene was monitored by TLC), the mixture was cooled to room temperature. The mixture was directly filtered and the product was afforded through column chromatograph eluting with hexane/ethyl acetate.

2　Results and discussion

2.1　Characterization of $[M_2L_2]^{2+}$-type coordination "clips"

The complexes were characterized by electrospray ionization mass spectrometry, NMR spectroscopy, IR spectroscopy and elemental analysis.

As shown in ^{1}H NMR spectra of $[M_2L_2]^{2+}$-type coordination "clips" (Fig. 1, 2, S5, S7~S9, S12~S15, S18 ~S21, S24, S25), the signals of protons of the complexes splited and shifted in comparison with those of the free ligands. The protons of the methyl of the flexible ligand shifted, showing only a single peak in free ligand before self-assembly. The protons of the NH of amide group in the flexible ligand shifted in comparision with free ligand before self-assembly. This can be explained that the CH_2-protons and NH-protons of the flexible ligand in the complexes are located in asymmetric chemical environment, which demonstrate a highly symmetrical structure of the complex[28-30].

The NMR analysis of $\mathbf{C1}\cdot 2NO_3^-$ clearly showed that a 1∶1 (bpy)Pd to L^1 complex was formed. As shown in Fig.1, NH-proton of amide group in the ligand of the product turned out to be one singlet at δ=9.88, which presented one singlet at δ=9.89 for L^1-NH, respectively before self-assembly (Fig.S1). In addition, two CH_2-protons of the ligand of the product turned out to be two singlets at δ=4.61 and 4.60, which presented two singlets at δ=4.62 and 4.64 for L^1-CH_2, respectively before self-assembly. And the results of ^{13}C NMR spectroscopy (Fig.S7) agreed well with the analysis of ^{1}H NMR spectroscopy. The NMR analysis of $\mathbf{C1}\cdot 2PF_6^-$ also clearly showed that a 1∶1 (bpy)Pd to L^1 complex was formed. As shown in Fig.2, NH-proton of amide group in the ligand of the product turned out to be only three singlets at δ=9.90~9.86, which presented one singlet at δ= 9.89, respectively before self-assembly (Fig. S1). In addition, two CH_2-protons in the ligand of the product
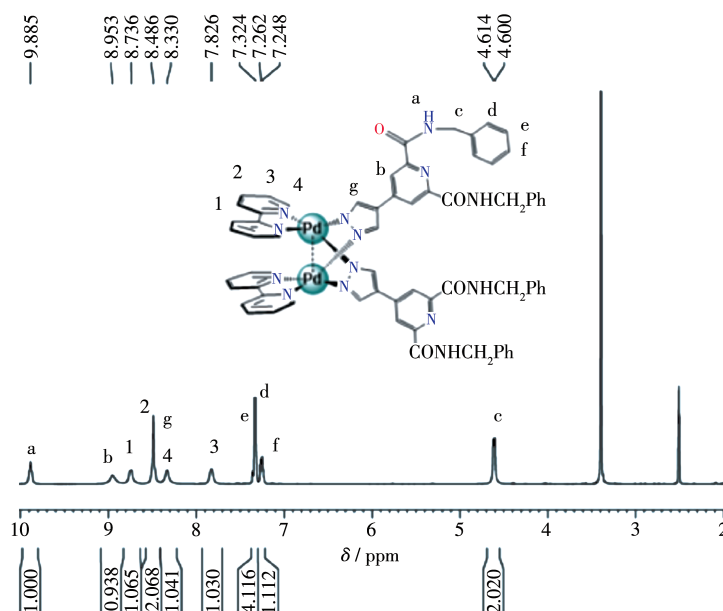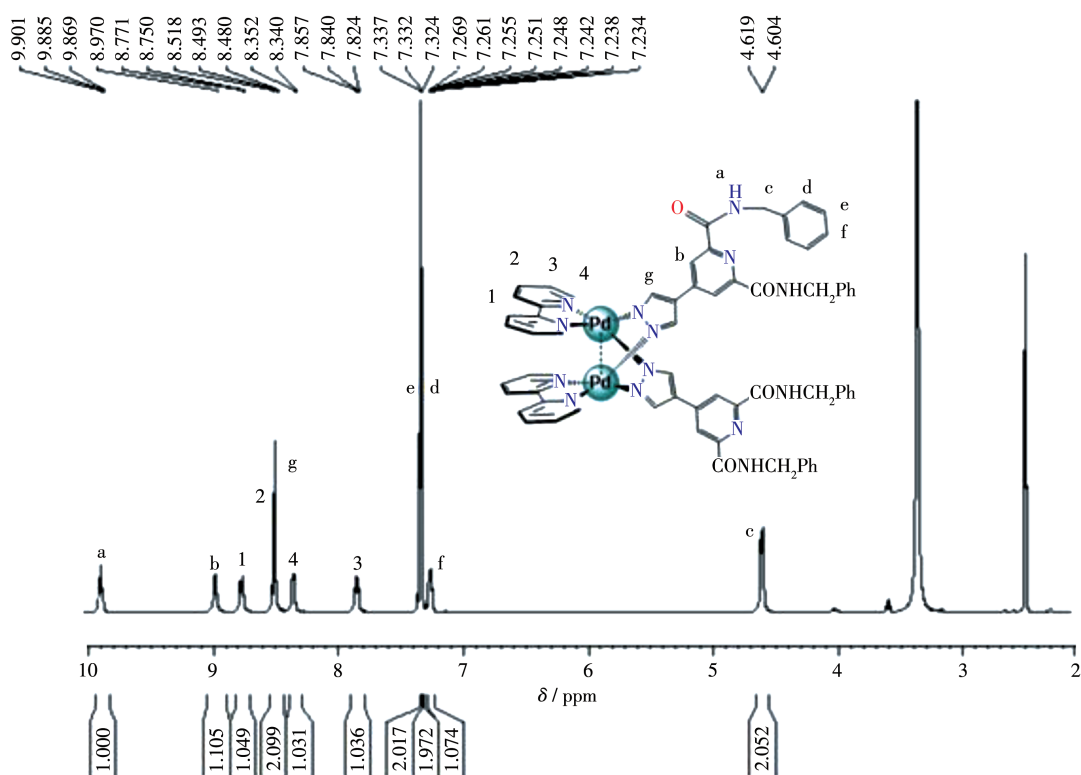

Fig.1　^{1}H NMR spectrum of $\mathbf{C1}\cdot 2NO_3^-$

Fig.2　^{1}H NMR spectrum of **C1**·2PF$_6^-$

turned out to be two singlets at δ=4.61 and 4.60, which presented two singlets at δ=4.62 and 4.64 for L^1-CH$_2$, respectively before self-assembly. And the results of ^{13}C NMR spectroscopy (Fig.S5) agreed well with the analysis of ^{1}H NMR spectroscopy. In the FT-IR spectrum of **C1**·2NO$_3^-$, the absorption bands in the region of 3 200~3 400 cm^{-1} can be attributed to the stretching vibrations of N—H. The bands in the region of 2 895~ 3 010 cm^{-1} can be ascribed to C—H stretching vibra-

tions of the benzene ring. The absence of the absorption bands at 1 450~1 600 cm^{-1} can be ascribed to C— C stretching vibrations of the benzene ring. Moreover, the assignment of product **C1**·2PF$_6^-$ as [M$_2$L$_2$]$^{2+}$-type dimetallo-clip was further proved by ESI-MS studies where multiply charged molecular ions corresponding to intact dimetallo-clip were observed. As shown in Fig.3, the multiply charged molecular ions of **C1**·2PF$_6^-$ at m/z=672.58, 1 490.90 are ascribed to the cations of
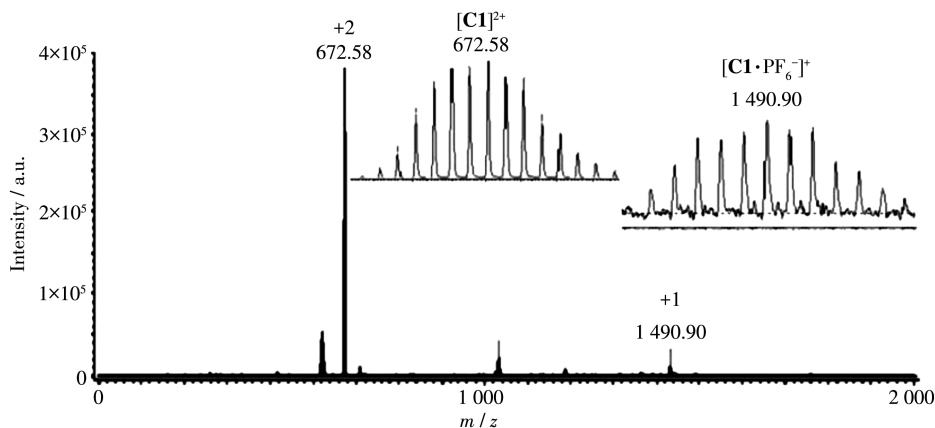
Inset: isotopic distribution of species [**C1**·PF$_6^-$]$^+$ and [**C1**]$^{2+}$

Fig.3　ESI-MS spectrum of **C1**·2PF$_6^-$ in acetonitrile

$[\mathbf{C1}]^{2+}$, $[\mathbf{C1} \cdot PF_6^-]^+$, respectively.

The NMR analysis of $\mathbf{C3} \cdot 2NO_3^-$ clearly showed that a 1:1 (bpy)Pd to L^1 complex was formed. As shown in Fig.S18, NH-proton of amide group in the ligand of the product turned out to be one singlet at δ =9.81, which presented one singlet at δ =9.89 for L^1 - NH, respectively before self-assembly (Fig.S1). In addition, two CH_2-protons in the ligand of the product turned out to be two singlets at δ=4.60 and 4.59, which presented two singlets at δ=4.62 and 4.64 for L^1-CH_2, respectively before self-assembly. And the results of ^{13}C NMR spectroscopy (Fig. S19) agreed well with the analysis of ^{1}H NMR spectroscopy. The NMR spectrum of $\mathbf{C3} \cdot 2PF_6^-$ clearly shows that a 1:1 (bpy)Pd to L^2 complex was formed. As shown in Fig.S14, NH-proton of amide group in the ligand of the product turned out to be only one singlet at δ=9.81, which presented one singlet at δ=9.96, respectively before self - assembly (Fig. S3). In addition, two CH_2-protons in the ligand of the product turned out to be two singlets at δ=4.59 and 4.60, which presented two singlets at δ=4.61 and 4.63 for HL^2-CH_2 before self-assembly; three CH_3-protons in the ligand of the product turned out to be one singlet at δ =2.69, which presented one singlet at δ =2.33 for HL^2 - CH_3 before self-assembly. And the results of ^{13}C NMR spectroscopy agreed well with the analysis of ^{1}H NMR spectroscopy (Fig. S15). In the FT - IR spectrum of $\mathbf{C3} \cdot 2NO_3^-$, the absorption bands in the region of 3 100~3 350 cm^{-1} can be attributed to the stretching vibrations of N—H. The bands in the region of 2 870~3 000 cm^{-1} can be ascribed to C—H stretching vibrations of the benzene ring. The absence of the absorption bands at 1 650~1 450 cm^{-1} can be ascribed to C—C stretching vibrations of the benzene ring. Moreover, the assignment of product $\mathbf{C3} \cdot 2PF_6^-$ as $[M_2L_2]^{2+}$-type dimetallo - clip was further proved by ESI - MS studies where multiply charged molecular ions corresponding to intact dimetallo-clip were observed. As shown in Fig. S13, the multiply charged molecular ions of $\mathbf{C3} \cdot 2PF_6^-$ at m/z=701.12, 1 547.21 are ascribed to the cations of $[\mathbf{C3}]^{2+}$, $[\mathbf{C3} \cdot PF_6^-]^+$, respectively.

The other four similar complexes $\mathbf{C2} \cdot 2PF_6^-$, $\mathbf{C2} \cdot 2NO_3^-$, $\mathbf{C4} \cdot 2NO_3^-$ and $\mathbf{C4} \cdot 2PF_6^-$ are also obtained and characterized by the similar method (Fig. S8~S13,

S20~S25). All the characterizations have demonstrated that the preparation of these organometallic clips as mentioned was successful which have similar molecular structures composed of two Pd(Ⅱ) motifs and two monoanionic ligands. The highly symmetrical structures of the $[M_2L_2]^{2+}$ - type of these "molecular clips" have been further confirmed by single-crystal X-ray diffraction analysis.

2.2 Crystal structure of dimetallo complex C1· $2NO_3^-$

The structure of complex $\mathbf{C1} \cdot 2NO_3^-$ was successfully determined by X - ray diffraction as depicted in Fig. 4, and labeled ORTEP plots of the cation of the complex are shown in Fig.S1. $\mathbf{C1} \cdot 2NO_3^-$ crystallizes in the space group $P\overline{1}$. The structure reveals a Pd_2 dimetallic clip-shaped structure with two functional ligands doubly bridged $[Pd(bpy)]_2$ dimetal "clip". The $[Pd_2L_2]$-type "clip" is supported by two pyrazolate ligands and one $[Pd_2(bpy)_2]$ motifs (Fig.4a and 4b). The central six-membered ring consists of two Pd(Ⅱ) ions and the four pyrazolyl N atoms has a boat-shaped conformation with Pd-N_{pz} distances between 0.19 and 0.20 nm. The Pd1··· Pd2 separation is 0.343 nm and the dihedral angle between the planes of two bpy ligands in the "clip" is 118.0°. The deprotonated ligands (L^1) are nearly perpendicular to each other, and the dihedral angle is 105.6° between the planes of pyrazolate groups. And this arrangement creates an "open book" disposition for the square-planar environment of two Pd(Ⅱ) ions. As shown in Fig.4c and 4d, dimetallic coordination "clip" can stack into a three-dimensional structure via strong multiple hydrogen bonding and weak $\pi \cdots \pi$ stacking interactions. Three intermolecular hydrogen bonds are formed between oxygen acceptors O6, O7 from nitrate anions and amide N donors (N9, N11, N12 and N14). The distances of O···H are 0.211 nm (O7···H12— N12) and 0.224 nm (O7···H14—N14), respectively. In this hydrogen bonding moieties, intramolecular N··· H—N bonds are also formed with an average separation of 0.230 nm. The two benzene rings in the complex are parallel, and the distances of the two rings range from 0.513 to 0.520 nm.

O7···H12　0.224 1 nm
O7···H14　0.211 5 nm
O9···H9　0.208 1 nm
O9···H11　0.208 8 nm
O6···H3　0.250 7 nm
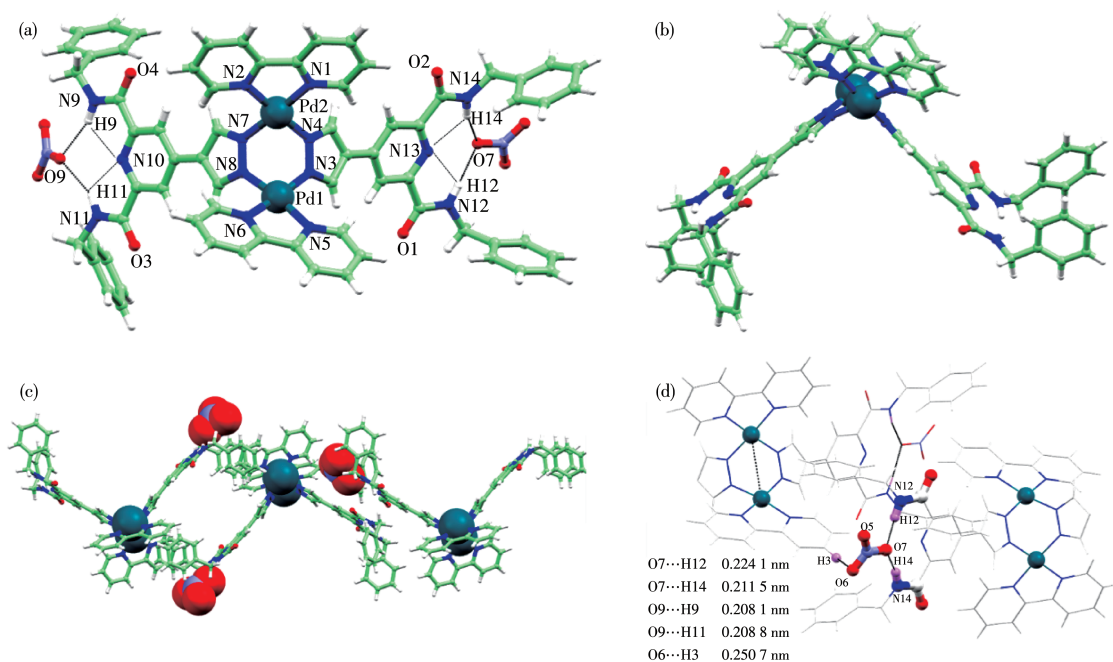
All the solvent molecules are omitted for clarity; Purple: Pd; Green and gray: C; Light grey and pink: H; Blue: N; Red: O

Fig.4　Crystal structure of **C1**·2NO$_3^-$: top view (a), side view (b), stacking mode (c); Multiple hydrogen bond interaction modes between nitrate and ligands (d)

2.3　Catalytic activity

It is well accepted that catalysts containing multiple metal centers in close proximity to each other can lead to better reactivity than the equivalent mixtures of monometallic complexes. In addition, dimetallic catalysts afford a higher nonlocal concentration of the activesites, and this may also lead to better catalytic performance than those of the analogous monometallic catalysts[31-32].

As shown in the Table 2, the free ligands HL^1 and HL^2 showed no catalytic activity to Suzuki-coupling reaction of iodobenzene and 3,4-dimethoxy benzeneboronic acid. Meanwhile, the reaction provide product in good yields for **C1**·2NO$_3^-$ ~**C4**·2NO$_3^-$ and **C1**·2PF$_6^-$ ~**C4**·2PF$_6^-$. This marked difference in catalytic activity may be attributed to the tunable impact and Pd(Ⅱ)···Pd(Ⅱ)

Table 2　Catalytic activity of as-prepared catalysts for Suzuki-coupling reaction of iodobenzene and 3,4-dimethoxy benzeneboronic acid

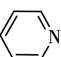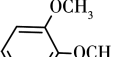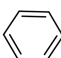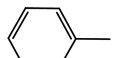| Entry*	Catalyst	Yield / %
1	[(dmbpy)$_2$Pd$_2$(NO$_3$)$_2$](NO$_3$)$_2$	65.4
2	[(bpy)$_2$Pd$_2$(NO$_3$)$_2$](NO$_3$)$_2$	66.7
3	HL^1	No reaction
4	HL^2	No reaction
5	**C1**·2NO$_3^-$	89.1
6	**C2**·2NO$_3^-$	87.1
7	**C3**·2NO$_3^-$	87.3
8	**C4**·2NO$_3^-$	86.5
9	**C1**·2PF$_6^-$	82.7
10	**C2**·2PF$_6^-$	82.4
11	**C3**·2PF$_6^-$	82.5
12	**C4**·2PF$_6^-$	83.1
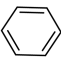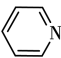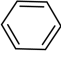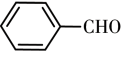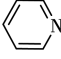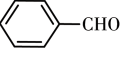
* Reaction conditions: co-catalyst: K$_3$PO$_4$, solvent: 1,4-dioxane, temperature: 100 ℃, time: 24 h.

intramolecular bonding interaction between the two Pd(Ⅱ) centers. In order to expand the scopes of reaction substrates, six different iodine-substituted and boronic acid-substituted aromatic compounds were chosen to react under the similar condition (Table 3 and S3). In these cases, the desirable products were obtained in high yields, signifying the excellent catalytic activities of $C1 \cdot 2NO_3^- \sim C4 \cdot 2NO_3^-$ and $C1 \cdot 2PF_6^- \sim C4 \cdot 2PF_6^-$.

Table 3 Scope of dimetal complex $C1 \cdot 2NO_3^-$ catalyst for Suzuki-coupling reactions

$$R_1 - I \ + \ \overset{HO}{\underset{HO}{\diagdown}} B - R_2 \ \xrightarrow[K_3PO_4, \ 1,4\text{-dioxane}, \ 100\ ℃]{Catalyst} \ R_1 - R_2$$

Entry*	Catalyst	R₁	R₂	Yield / %
1	$C1 \cdot 2NO_3^-$	(phenyl)	(pyridyl, N)	81.6
2	$C1 \cdot 2NO_3^-$	(phenyl)	(phenyl)	99.0
3	$C1 \cdot 2NO_3^-$	(phenyl)	(phenyl)—CHO	80.1
4	$C1 \cdot 2NO_3^-$	(pyridyl, N)	(phenyl)—CHO	77.8
5	$C1 \cdot 2NO_3^-$	(pyridyl, N)	(phenyl with OCH₃, OCH₃)	81.5
6	$C1 \cdot 2NO_3^-$	(phenyl)	(phenyl)—	92.5

* Reaction conditions: co-catalyst: K_3PO_4, solvent: 1,4-dioxane, temperature: 100 ℃, time: 24 h.

3 Conclusions

In conclusion, two ditopic carboxamide-pyrazolate ligands were synthesized and used to construct novel pyrazolate-bridged dipalladium coordination "clips" $C1 \cdot 2NO_3^- \sim C4 \cdot 2NO_3^-$ and $C1 \cdot 2PF_6^- \sim C4 \cdot 2PF_6^-$ with strong Pd(Ⅱ)···Pd(Ⅱ) bonding interaction. The coordination "clips" ($C1 \cdot 2NO_3^-$) can trap two nitrate anions via multiple N—H···O hydrogen bonds in the semi-open cavity composed of two amide groups. The complexes were characterized by elemental analysis, NMR, ESI-Ms and IR spectroscopy. Moreover, these pyrazolate-based dipalladium "clips" containing a dimetal active center exhibited good catalytic activity for Suzuki-coupling reaction.

Supporting information is available at http://www.wjhxxb.cn

References:

[1] Chakrabarty R, Mukherjee P S, Stang P J. *Chem. Rev.*, **2011,111**:6810 -6918

[2] Fujita M, Tominaga M, Hori A, Therrien B. *Acc. Chem. Res.*, **2005,38**: 369-378

[3] Sun Y, Chen C, Liu J, Stang P J. *Chem. Soc. Rev.*, **2020,49**:3889-3919

[4] He L P, Wang S C, Lin L T, Cai J Y, Li L J, Tu T H, Chan Y T. *J. Am. Chem. Soc.*, **2020,142**:7134-7144

[5] Zaffaroni R, Bobylev E O, Plessius R, Vlugt J I V D, Reek J N H. *J. Am. Chem. Soc.*, **2020,142**:8837-8847

[6] Qin J H, Zhang H, Sun P, Huang Y D, Shen Q, Yang X G, Ma L F. *Dalton Trans.*, **2020,49**:17772-17778

[7] Wang S, Sawada T, Fujita M. *Chem. Commun.*, **2016,52**:11653-11656

[8] Therrien B. *Chem. Eur. J.*, **2013,19**:8378-8386

[9] Cullen W, Thomas K A, Hunter C A, Ward M D. *Chem. Sci.*, **2015,6**: 4025-4028

[10]Schmitt F, Freudenreich J, Barry N P E, Juillerat J L, Süss F G, Therrien B. *J. Am. Chem. Soc.*, **2012,134**:754-757

[11]Isklan M, Saeed M A, Pramanik A, Wong B M, Fronczek F R, Hossain M A. *Cryst. Growth Des.*, **2011,11**:959-963

[12]Langton M J, Duckworth L C, Beer P D. *Chem. Commun.*, **2013,49**: 8608-8610

[13]Qin J H, Huang Y D, Zhao Y, Yang X G, Li F F, Wang C, Ma L F. *Inorg. Chem.*, **2019,58**:15013-15016

[14]Du X S, Yan B J, Wang J Y, Xi X J, Wang Z Y, Zang S Q. *Chem. Commun.*, **2018,54**:5361-5364

[15]Zhou L P, Sun Q F. *Chem. Commun.*, **2015**,**51**:16767-16770

[16]Jiang X F, Hau F K W, Sun Q F, Yu S Y, Yam V W W. *J. Am. Chem. Soc.*, **2014**,**136**:10921-10929

[17]Qin J H, Wang H R, Pan Q, Zang S Q, Hou H, Fan Y. *Dalton Trans.*, **2015**,**44**:17639-17651

[18]Chen Z M, Cui Y, Jiang X F, Tong J, Yu S Y. *Chem. Commun.*, **2017**, **53**:4238-4241

[19]Tong J ,Yu S Y, Li H. *Chem. Commun.*, **2012**,**48**:5343-5345

[20]Baya M, Houghton J, Konya D, Champouret Y, Daran J C, Lenero K Q A, Schoon L, Mul W P, Oort B V, Meijboom N, Drent E, Orpen A G, Poli R. *J. Am. Chem. Soc.*, **2008**,**130**:10612-10624

[21]Oldenhof S, Lutz M, Bruin B, Vlugt J I, Reek J N. *Organometalics*, **2014**,**33**:7293-7298

[22]Sun W Q, Tong J, Lu H L, Ma T T, Ma H W, Yu S Y. *Chem. Asian J.*, **2018**,**13**:1108-1113

[23]陈涵, 于智淳, 邓威, 蒋选丰, 于澍燕. 无机化学学报, **2017**,**33**(6): 939-946

CHEN H, YU Z C, DENG W, JIANG X F, YU S Y. *Chinese J. Inorg. Chem.*, **2017**,**33**(6):939-946

[24]胡佳华, 邓威, 蒋选丰, 于澍燕. 无机化学学报, **2015**,**31**(7):1278-1286

HU J H, DENG W, JIANG X F, YU S Y. *Chinese J. Inorg. Chem.*, **2015**,**31**(7):1278-1286

[25]张忠兴, 黄辉, 于澍燕. 无机化学学报, **2004**,**20**(7):849-852

ZHANG Z X, HUANG H, YU S Y. *Chinese J. Inorg. Chem.*, **2004**,**20**(7):849-852

[26]Cui Y, Chen Z M, Jiang X F, Tong J, Yu S Y. *Dalton Trans.*, **2017**, **46**:5801-5805

[27]Sheldrick G M. *Acta Crystallogr. Sect. C*, **2015**,**C71**:3-8

[28]Bratko I, Gomez M. *Dalton Trans.*, **2013**,**42**:10664-11081

[29]Fr Ⅱ s S D, Pirnot M T, Dupuis L N, Buchwald S L. *Angew. Chem. Int. Ed.*, **2017**,**56**;7242-7724

[30]Qin J H, Wang H R, Han M L, Chang X H, Ma L F. *Dalton Trans.*, **2017**,**46**:15434-15442

[31]Reek J N H, Arevalo S, Heerbeek R V, Kamer P C J, Leeuwen P V. *Advances in Catalysis*: *Vol*.49. Amsterdam: Academic Press, **2006**:71-151

[32]Helms B, Frechet J M J. *Adv. Synth. Catal.*, **2006**,**348**:1125-1148